

# A novel organic chromophore for dye-sensitized nanostructured solar cells†

Daniel P. Hagberg,<sup>a</sup> Tomas Edvinsson,<sup>\*b</sup> Tannia Marinado,<sup>b</sup> Gerrit Boschloo,<sup>b</sup> Anders Hagfeldt<sup>b</sup> and Licheng Sun<sup>\*a</sup>

Received (in Cambridge, UK) 28th February 2006, Accepted 30th March 2006

First published as an Advance Article on the web 13th April 2006

DOI: 10.1039/b603002e

A novel and efficient polyene-diphenylaniline dye for dye-sensitized solar cells has been synthesized. The dye has a short synthesis route and is readily adsorbed on TiO<sub>2</sub> under a variety of dye-bath conditions. The overall solar-to-energy conversion efficiency is over 5% in the preliminary tests, in comparison with the conventional N719 dye which gives 6% under the same conditions. The dye is designed for future use also in solid state devices, with triarylamine based hole conductors.

Dye-sensitized solar cells (DSSCs) have attracted a lot of interest for their abilities to convert solar light to electricity at low cost. Dyes of Ru complexes such as the N3/N719 dye<sup>1,2</sup> and the black dye<sup>3</sup> have been intensively investigated, and show record solar-energy-to-electricity conversion efficiencies ( $\eta$ ) of 11% under AM 1.5 irradiation.<sup>4</sup> Studies of Ru dyes with other electron-donor groups, such as diphenylaniline have shown interesting results promising for DSSC applications.<sup>5,6</sup> The interest in metal free, organic dyes with high extinction coefficients has grown in recent years. The organic dyes for DSSCs based on diphenylaniline as electron donor, published so far, include relatively complicated synthetic procedures, such as Stille or Suzuki couplings or more steps in the synthetic route.<sup>7,8</sup> In order to investigate organic dyes and, in the longer run, prepare an efficient solar cell dye, a number of different organic dyes were designed and synthesized. Here we present an efficient dye that is easily synthesized and can be produced at low cost due to the short synthetic route.

In this dye (D5) the diphenylaniline moiety acts as an electron donor and the cyanoacetic moiety acts as the electron acceptor and as anchoring groups for attachment on the TiO<sub>2</sub> (see Fig. 1). The thiophene chain extends the  $\pi$ -conjugation and thereby gives a red shift in the absorption spectrum without affecting the stability of the dye.<sup>9</sup> An extended  $\pi$ -conjugation with a methine chain would probably give a red shift of the absorption peak, but would also complicate the synthetic procedure and affect the stability of the dye due to possible isomer formation. To obtain a dye with efficient photocurrent generation,  $\pi$ -stacked aggregation on the TiO<sub>2</sub> should normally be avoided.<sup>10</sup> Aggregation may lead to intermolecular quenching or molecules residing in the system not functionally attached to the TiO<sub>2</sub> surface and thus acting as filters.

<sup>a</sup>Center of Molecular Devices, Organic Chemistry, Royal Institute of Technology, Teknikringen 30, 10044, Stockholm, Sweden.

E-mail: lichengs@kth.se; Fax: +46 8 791 2333; Tel: +46 8 790 8127

<sup>b</sup>Center of Molecular Devices, Physical Chemistry, Royal Institute of Technology, Teknikringen 30, 10044, Stockholm, Sweden.

E-mail: tomased@kth.se; Fax: +46 8 790 8207; Tel: +46 8 790 8178

† Electronic supplementary information (ESI) available: Experimental details. See DOI: 10.1039/b603002e

The diphenylaniline moiety is non-planar and would suppress aggregation due to the disturbance of the  $\pi$ - $\pi$  stacking.

The three step synthesis of the dye includes well known reactions and gives a moderate yield. The thiophene moiety was coupled to 4-(diphenylamino)benzaldehyde accordingly to the Wittig reaction, followed by formylation of the thiophene functionality.<sup>11</sup> Finally condensation of the aldehyde with cyanoacetic acid by the Knoevenagel reaction in the presence of piperidine: an acetonitrile (MeCN) solution of 5-(2-(4-diphenylamino-phenyl)-vinyl)-thiophene-2-carbaldehyde and cyanoacetic acid was refluxed in the presence of piperidine for 4 h. Solvent removal by rotary evaporator followed by purification by column chromatography

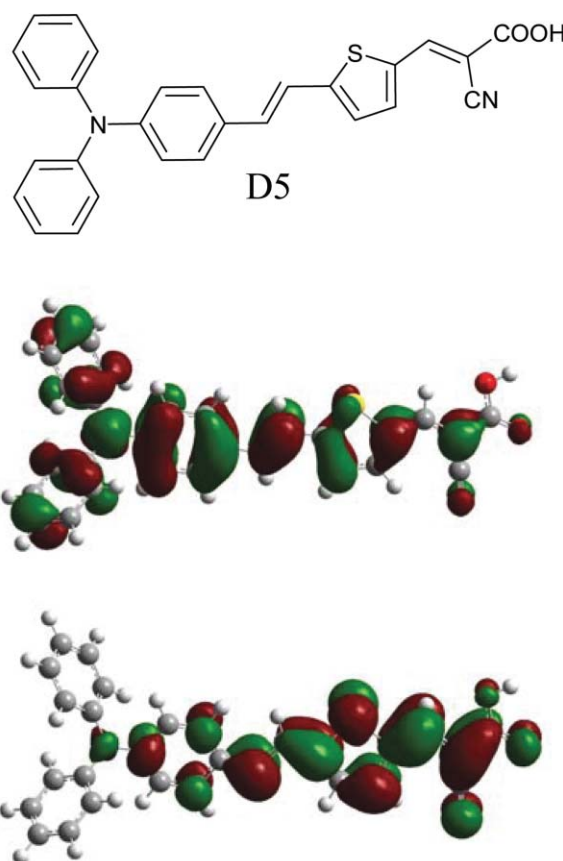


**Fig. 1** The molecular structure of the novel D5 dye (top) and the frontier molecular orbitals of the HOMO (middle) and LUMO (bottom) calculated with TD-DFT on a B3LYP/6-31 + G(d) level. The redistribution of electron densities shows the pronounced push-pull characteristics of the dye, giving an efficient intramolecular charge separation.

yielded a dark purple solid. For details, see the electronic supplementary information.†

Nanostructured TiO<sub>2</sub> (anatase) photoelectrodes were prepared by screen printing a colloidal solution onto a conducting glass (Pilkington TEC15, fluorine-doped SnO<sub>2</sub> glass with a sheet resistance of 15 Ω/square). The TiO<sub>2</sub> screen printing paste was prepared by hydrolysis of titanium tetraisopropoxide<sup>12</sup> with the addition of ethyl cellulose as binder in α-terpineol. A second, scattering, layer was deposited with doctor blading technique. The latter TiO<sub>2</sub> paste was prepared with 50/50%w of 10 nm TiO<sub>2</sub> particles (synthesized as above) and 300 nm TiO<sub>2</sub> particles (Bayertitan, silica covered), blended with polyethyleneglycol ( $M_w = 20\,000\text{ g mol}^{-1}$ ) in water. The resulting photoelectrodes of 10 + 6 μm thickness, were sintered at 490 °C for 40 min and then immersed into a 1 mM dye solution in MeCN. The photovoltaic measurements were performed with the dye-coated TiO<sub>2</sub> electrode sealed with a 50 μm thick Surlyn frame and a counter electrode with nanoparticulate platinum on a conducting glass. The 0.48 cm<sup>2</sup> solar cell was mounted on a frame, masking the solar cell to 0.32 cm<sup>2</sup>. The electrolyte consisted of 0.6 M tetrabutylammonium iodide (TBAI), 0.1 M LiI, 0.05 M I<sub>2</sub>, 0.5 M 4-*tert*-butylpyridine (4-TBP) in MeCN. The photovoltage–photocurrent measurements were performed with a sulfur lamp setup calibrated to AM 1.5.‡ UV-vis and fluorescence spectra of the dye in acetonitrile show two absorption bands with absorption maxima at 476 nm and 300 nm (see Fig. 2). The extinction coefficient,  $\epsilon(\lambda)$ , was determined to 37 600 M<sup>-1</sup>cm<sup>-1</sup> at the absorption maximum 476 nm in acetonitrile, giving the mass extinction coefficient 84 g<sup>-1</sup>cm<sup>-1</sup>. When the dye is attached to TiO<sub>2</sub>, a blue shift of the absorption maximum from 476 nm to 444 nm was found, not changing when adding acetonitrile on the TiO<sub>2</sub>/dye slide. The blue shift thus originates from the interaction with TiO<sub>2</sub>. In methanol the dye has an absorption maximum at 444 nm indicating that the blue shift on TiO<sub>2</sub> is a shift arising from a polar interaction and/or



**Fig. 2** Absorption (---) and emission spectra (—) of the D5 dye in MeCN compared with the absorption spectrum of the dye attached to TiO<sub>2</sub> (···). The excitation wavelength for emission was 460 nm. The absorption and emission maxima in MeCN are 476 nm and 625 nm giving a Stokes shift of 0.62 eV and a zeroth–zeroth transition  $\Delta E_{0-0} = 2.25\text{ eV}$ . The absorption maximum of the dye attached to the TiO<sub>2</sub> nanoparticles is blue shifted to 444 nm.

deprotonation. Addition of acid (acetic acid) in methanol redshifts the spectrum to 474 nm, revealing that the blue shift in methanol is mainly originating from the deprotonation. The solvatochromic behavior of the dye and the specific interaction with metal oxides will be studied in a forthcoming publication.

Density functional theory (DFT) calculations were made in gas phase on a B3LYP/6-31 + G(d) level with Gaussian 03.<sup>13</sup> Time dependent DFT excited state calculations gave two transitions with large oscillator strengths ( $f$ ), consistent with the absorption spectrum. A HOMO→LUMO transition with transition energy 2.26 eV (548 nm) with  $f = 1.17$  and a combined transition: HOMO-1→LUMO and HOMO→LUMO+1 with 3.10 eV (399 nm) and  $f = 0.78$ . Estimating the absorption coefficient for the strongest transition, assuming a Gaussian profile of the bands and taking the width from the UV-vis spectrum we arrive at  $\epsilon = 45\,000\text{ M}^{-1}\text{cm}^{-1}$  for the strongest transition. Since this is in gas phase and for a dye with pronounced solvatochromism, we expect both a damping of the absorption efficiency and a blue shift of the bands when going to polar solvents such as MeCN. The electronic redistribution between the HOMO and LUMO (depicted in Fig. 1) show a pronounced intramolecular charge separation for this transition. Assuming similar molecular orbital geometry when anchored to TiO<sub>2</sub>, the position of the LUMO close to the anchoring group will enhance the orbital overlap with the titanium 3d orbitals and favour electron injection.

Cyclic voltammetry (CV) and square wave voltammetry (SWV) were employed to measure the oxidation and reduction potentials of the dye, see Fig. 3. The measurements were performed in dry MeCN (Fluka >99.9%) with 0.1 M tetrabutylammonium hexafluorophosphate (TBAPF<sub>6</sub>) as supporting electrolyte. The reference electrode was a silver wire calibrated with Ferrocene/Ferrocenium (Fc/Fc<sup>+</sup>) as an internal reference. The oxidation potential was determined to 450 mV and the reduction potential to -1550 mV vs. Fc/Fc<sup>+</sup> (1080 mV and -920 mV vs. NHE, respectively), an oxidation potential energetically favourable for

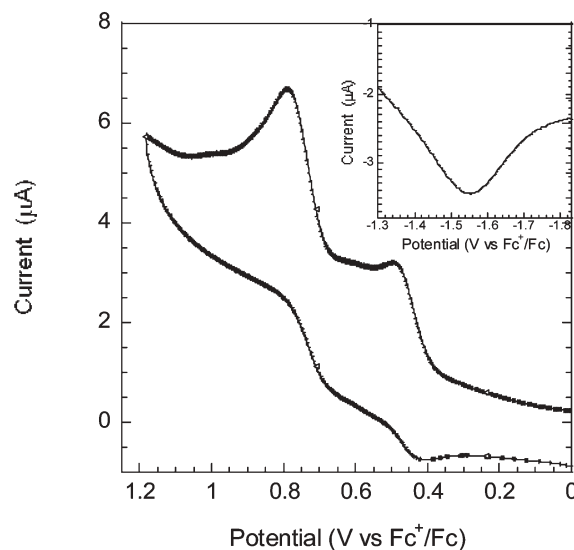


**Fig. 3** Cyclic voltammogram of the oxidation behaviour and square wave voltammogram (inset) of the reduction, measured at a scan rate of 100 mV s<sup>-1</sup>. The formal potentials of oxidation and reduction were determined to 450 mV and -1550 mV vs. Fc<sup>+</sup>/Fc.



**Fig. 4** IPCE spectra for dye sensitized TiO<sub>2</sub> solar cells with (---) and without scattering layer (—). The electrolyte was 0.6 M TBAI, 0.1 M LiI, 0.05 M I<sub>2</sub>, and 0.5 M 4-TBP in MeCN.

iodide oxidation. Estimating the HOMO energy in MeCN from the formal potential of oxidation (thus neglecting the reorganization energy) and adding the zeroth-zeroth energy  $\Delta E_{0-0} = 2.25$  eV (taken from Fig. 2) we arrive at  $-1.17$  V vs. NHE for the LUMO. This is well above the conduction band level of TiO<sub>2</sub> at approximately  $-0.5$  V vs. NHE. The photovoltaic performance was measured at  $1000 \text{ W m}^{-2}$  under AM 1.5 conditions. For the best cell, the overall solar-to-electric conversion efficiency was 5.1% (with short-circuit photocurrent density  $J_{sc} = 11.9 \text{ mA cm}^{-2}$ , open-circuit photovoltage  $V_{oc} = 0.66$  V, fill factor  $ff = 0.68$ ). Overall efficiencies of 4–5% for a variety of dye bath conditions (1 mM, 170  $\mu\text{M}$ , with and without deoxycholic acid) were obtained. This can be compared to solar cells with the conventional ruthenium dye N719 made under similar conditions (with dye baths in ethanol optimized for the N719 dye) giving  $\eta = 6.1$ –6.4%.

Measuring the incident to photon current efficiency (IPCE), the highest values obtained for D5 were 85% at 400 nm and 70–65% at the plateau between 450–600 nm for an electrolyte without the additive 4-*tert*-butyl pyridine (4-TBP). Fig. 4 displays typical IPCE curves with 4-TBP where the IPCE values are only slightly lower with this photovoltage-increasing additive. A 10  $\mu\text{m}$  dye sensitized TiO<sub>2</sub> solar cell with and without a scattering layer are compared, where a slight improvement of the photoresponse in the red region of the IPCE spectrum is seen for the solar cell with scattering layer (6% increase in total photocurrent). The high extinction coefficient of this dye allows for the use of thinner TiO<sub>2</sub> films which are required in solid state devices.<sup>14</sup>

The results show promise for future use in nanostructured dye-sensitized solar cells with respect to low materials costs, high

performance, and recyclability. The donor group is also of interest for use in nanostructured solid state cells based on organic hole conductors.

We acknowledge the Swedish Research Council, Swedish Energy Agency, and BASF AG Ludwigshafen for financial support. The authors would also like to thank Ms Rong Zhang at Dalian University of Technology, China, for the mass spectroscopy measurements, and Dr. Xichuan Yang (Dalian) and Professor Björn Åkermark at Stockholm University are thanked for discussions.

## Notes and references

‡ The total integrated photocurrent from the IPCE measurements was used to adjust the power of the sulfur lamp setup to give the same short circuit photocurrent. The results were further certified by measurements in a Xe-lamp with a Tempax 113 filter calibrated with a reference solar cell.

- 1 M. K. Nazeeruddin, A. Kay, I. Rodicio, R. Humphry-Baker, E. Muller, P. Liska, N. Vlachopoulos and M. Gratzel, *J. Am. Chem. Soc.*, 1993, **115**, 6382–6390.
- 2 M. K. Nazeeruddin, S. M. Zakeeruddin, R. Humphry-Baker, M. Jirousek, P. Liska, N. Vlachopoulos, V. Shklover, C. H. Fischer and M. Gratzel, *Inorg. Chem.*, 1999, **38**, 6298–6305.
- 3 M. K. Nazeeruddin, P. Pechy, T. Renouard, S. M. Zakeeruddin, R. Humphry-Baker, P. Comte, P. Liska, L. Cevey, E. Costa, V. Shklover, L. Spiccia, G. B. Deacon, C. A. Bignozzi and M. Gratzel, *J. Am. Chem. Soc.*, 2001, **123**, 1613–1624.
- 4 M. Gratzel, *J. Photochem. Photobiol., A*, 2004, **168**, 235–235.
- 5 S. A. Haque, S. Handa, K. Peter, E. Palomares, M. Thelakkat and J. R. Durrant, *Angew. Chem., Int. Ed.*, 2005, **44**, 5740–5744.
- 6 J. E. Moser, *Nat. Mater.*, 2005, **4**, 723–724.
- 7 T. Kitamura, M. Ikeda, K. Shigaki, T. Inoue, N. A. Anderson, X. Ai, T. Lian and S. Yanagida, *Chem. Mater.*, 2004, **16**, 1806–1812.
- 8 M. Velusamy, K. R. J. Thomas, J. T. Lin, Y. C. Hsu and K. C. Ho, *Org. Lett.*, 2005, **7**, 1899–1902.
- 9 K. Hara, M. Kurashige, Y. Dan-oh, C. Kasada, A. Shinpo, S. Suga, K. Sayama and H. Arakawa, *New J. Chem.*, 2003, **27**, 783–785.
- 10 Z. S. Wang, F. Y. Li, C. H. Huang, L. Wang, M. Wei, L. P. Jin and N. Q. Li, *J. Phys. Chem. B*, 2000, **104**, 9676–9682.
- 11 Z. Y. Hu, A. Fort, M. Barzoukas, A. K. Y. Jen, S. Barlow and S. R. Marder, *J. Phys. Chem. B*, 2004, **108**, 25, 8626–8630.
- 12 B. O'Regan and M. Graetzel, *Nature*, 1991, **353**, 6346, 737–740.
- 13 M. J. Frisch, G. W. Trucks, H. B. Schlegel, G. E. Scuseria, M. A. Robb, J. R. Cheesman, J. A. Montgomery, Jr., T. Vreven, K. N. Kudin, J. C. Burant, J. M. Millam, S. S. Iyengar, J. Tomasi, V. Barone, B. Mennucci, M. Cossi, G. Scalmani, N. Rega, G. A. Petersson, H. Nakatsuji, M. Hada, M. Ehara, K. Toyota, R. Fukuda, J. Hasegawa, M. Ishida, T. Nakajima, Y. Honda, O. Kitao, H. Nakai, M. Klene, X. Li, J. E. Knox, H. P. Hratchian, J. B. Cross, C. Adamo, J. Jaramillo, R. Gomperts, R. E. Stratmann, O. Yazyev, A. J. Austin, R. Cammi, C. Pomelli, J. W. Ochterski, P. Y. Ayala, K. Morokuma, G. A. Voth, P. Salvador, J. J. Dannenberg, V. G. Zakrzewski, S. Dapprich, A. D. Daniels, M. C. Strain, O. Farkas, D. K. Malick, A. D. Rabuck, K. Raghavachari, J. B. Foresman, J. V. Ortiz, Q. Cui, A. G. Baboul, S. Clifford, J. Cioslowski, B. B. Stefanov, G. Liu, A. Liashenko, P. Piskorz, I. Komaromi, R. L. Martin, D. J. Fox, T. Keith, M. A. Al-Laham, C. Y. Peng, A. Nanayakkara, M. Challacombe, P. M. W. Gill, B. Johnson, W. Chen, M. W. Wong, C. Gonzalez and J. A. Pople, *GAUSSIAN 03 (Revision B.03)*, Gaussian, Inc., Pittsburgh PA, 2003.
- 14 L. Schmidt-Mende, U. Bach, R. Humphry-Baker, T. Horiuchi, H. Miura, S. Ito, S. Uchida and M. Gratzel, *Adv. Mater.*, 2005, **17**, 813–815.